Long-Term VERITAS Monitoring and Multi-Wavelength Data on TXS 0506+056: Probing Intergalactic Cascades with VERITAS, *Swift*, and *Fermi* Observations

Connor Mooney, Atreya Acharyya, and Manuel Meyer on behalf of the VERITAS Collaboration

University of Delaware

comooney@udel.edu

Abstract

In September 2017, the IceCube Neutrino Observatory detected a high-energy neutrino event, IceCube170922A, associated with a gamma-ray flare from the blazar TXS 0506+056, with a probability of chance coincidence rejected at the 3σ level. This remains the most significant photon-neutrino correlation observed to date. Here, we present results from the long-term monitoring of TXS 0506+056 conducted by VERITAS, significantly expanding the observational coverage compared to previous studies. Data from *Swift* and *Fermi*-LAT further complement these observations. Using these comprehensive datasets, we compare the gamma-ray spectrum and neutrino observations to a model which uniquely includes a cosmic-ray induced cascade component in intergalactic space. We discuss the implications of these findings for understanding the proton injection spectrum and constraints on proton escape luminosity.

Introduction/Background

The origin of the diffuse astrophysical neutrino flux, detected by the IceCube Neutrino Observatory from TeV to PeV energies, remains unresolved in high-energy astrophysics [1]. High-energy neutrinos are produced through interactions between cosmic rays and ambient matter or photon fields, processes that also generate gamma rays, observable by instruments like the *Fermi* Large Area Telescope (LAT) and ground-based Cherenkov telescopes (IACTs) like VERITAS. Blazars—active galactic nuclei with jets aligned toward us—are proposed as significant contributors, as the isotropic distribution of the IceCube neutrino flux indicates a broader extragalactic origin, with blazars contributing up to 27% [2].

On September 22, 2017, IceCube detected a 290 TeV neutrino event, IceCube-170922A, whose direction matched the blazar TXS 0506+056 during a gamma-ray flare observed by Fermi-LAT [3]. This coincidence, with a chance probability of 3σ [4], supports the idea that blazars can accelerate cosmic rays, producing both neutrinos and gamma rays.

Beyond direct production at the source, cosmogenic neutrinos and gamma rays may arise from cosmic-ray interactions with the cosmic microwave background (CMB) and extragalactic background light (EBL). Specifically, cosmic rays can interact with background photons primarily via photopion production: $\mathbf{p+\gamma \rightarrow \Delta^{+} \rightarrow \pi^{0}+p}$; the π^0 decays immediately into two gamma rays, which can further interact with background photons (γ_{bg}) to produce electron-positron pairs: $\mathbf{\gamma+\gamma_{bg} \rightarrow e^{+}+e^{-}}$. These pairs can inverse Compton scatter background photons up to gamma-ray energies and subsequently initiate electromagnetic cascades [5].

This study extends the analysis of TXS 0506+056 using a comprehensive dataset from VERITAS, *Swift*, and *Fermi*-LAT, expanding the temporal coverage of previous research.

We compare the gamma-ray spectrum and neutrino observations with a model that includes escaped proton-induced cascades in intergalactic space. We perform a joint fit of the primary gamma-ray emission and the proton emission spectrum to constrain the escaped proton distribution as well as the proton escape luminosity.

Data Analysis

- VERITAS: an array of four 12-meter imaging atmospheric Cherenkov telescopes. Initial observations, conducted between September 2017 and February 2018, resulted in a detection at a significance of 5.8σ over 35 hours of data [6]. This is now reanalyzed with updated analysis tools during a flaring state of 25 hours to find a significance of **8.6σ**. Additional observations from October 2018 to March 2021, covering 61 hours, found the source in a quiescent state with a 3.4σ significance [7]. The average integrated flux above 0.15 TeV is **(5.987 ± 0.8954)×10^{-12} cm^{-2}s^{-1}** The VERITAS analysis used data from the flare period (MJD 58019 – MJD 58155) for our modelling, with only runs of the best weather conditions and high elevation accepted. The combined spectrum during the flare is best fit with a power-law of spectral index **4.91 ± 0.86**.

- Fermi-LAT: while the full dataset from MJD 54683 to 60218 was used for the lightcurve analysis (figure 1), data from MJD 58019 to MJD 58155 were used specifically for modeling the SED (figure 2) during the VERITAS flare in order to reflect the same physical state of the source. Photons between 100 MeV and 300 GeV within a 15° radius were selected. The data were processed using a binned maximum likelihood analysis, with sources within a 20° radius included in the model. The spectral shape parameters of sources within 3° were left free to vary. The analysis employed the latest PASS 8 IRFs with the Fermi Science Tools version 2.2.0 and FERMIPY version 1.2.2 [8]. TXS 0506+056 was detected with a significance of **45.4σ**, with a flux of **(2.3±0.2)×10^{-7} cm^{-2}s^{-1}** during flaring period. The spectrum was best modeled by a log parabola, with **Γ = 2.06 ± 0.02 and β = 0.05 ± 0.01**. Using the entire dataset of *Fermi*-LAT, we find a high significance of **129σ**.

- *Swift*-XRT: part of the Neil Gehrels Swift Observatory, observed TXS 0506+056 between August 2008 and October 2023 (MJD 54683–60218), accumulating 1370 ks of data in photon-counting mode. This data were analyzed using the HEASOFT v6.21 package [9] The average photon flux in the 0.3–10 keV range was (**2.36 ± 0.05) erg cm^{-2} s^{-1}**, with negligible photon pile-up. Individual spectra for each of the 114 observations, totaling ~46 hours, were fitted with an absorbed power-law model accounting for both Galactic and intrinsic absorption. The resulting combined spectrum has a spectral index of **2.039 ± 0.020**, and the flux was assessed using the cflux convolution model. The lightcurve, based on absorption-corrected flux values, shows variability over the observation period.

- *Swift*-UVOT: used to monitor TXS 0506+056 across 6 filters covering 2.3 to 6.1 eV, corresponding to UV and optical wavelengths, over multiple observation periods between MJD 55037 and MJD 59515. A total of 416 observations were performed, each analyzed using Python helper scripts that utilized the HEASOFT tool UVOTSOURCE for generating light curves. The analysis focused on a 5''-radius circular ON-region and a 20''-radius circular OFF-region for background subtraction. Approximately 45 images were removed due to imaging issues like slewing and readout streaks. The fluxes were corrected for Galactic extinction using E(B-V) = 0.092. Note that *Swift* data has not yet been used for our modelling, but included in our lightcurve in figure 1.

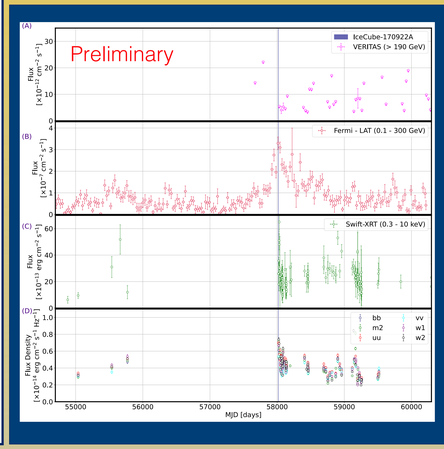

Figure 1: Multiwavelength lightcurves of TXS 0506+056 from MJD 54683 to 60218. The blue band marks the IceCube-170922A alert on MJD 58018. (A) VERITAS VHE lightcurve (>190 GeV) with monthly bins; 95% C.L. upper limits are shown for <2σ significance. (B) *Fermi*-LAT lightcurve (0.1–300 GeV) in 30-day bins; upper limits are shown for <2σ significance. (C) *Swift*-XRT flux points (0.3–10 keV) binned by "observation ID" (~1 day) (D) *Swift*-UVOT flux in the UV (UW1, UW2, UM2) and visible (U, B, V) filters also binned by "observation ID."

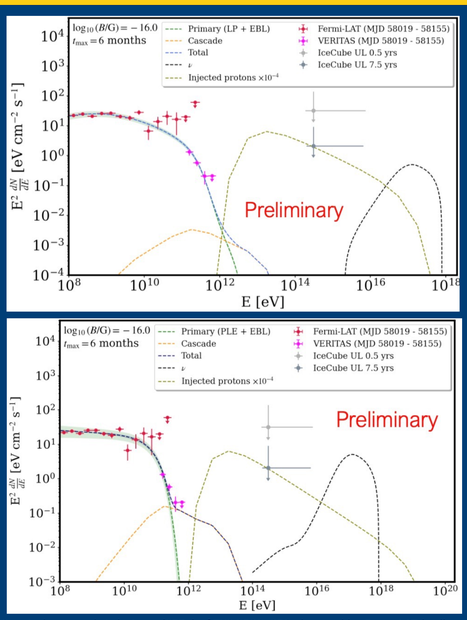

Figure 2: Spectral energy distributions (SEDs) of TXS 0506+056 observed by *Fermi*-LAT (red) and VERITAS (magenta), with the total best-fit spectrum shown by the dashed blue line. This total includes the primary spectra (above: LP + EBL, below: PLE + EBL, dashed green) and the cascade components (dashed orange). Spectral points below 2σ significance are marked as upper limits. The SEDs for proton injection (olive, scaled by 10^{-2} for visibility) and neutrinos (black) are also shown. Proton cascade and injection spectra correspond to specific parameters (α = 2.6, E_{max} = 3 × 10^{18} eV for LP; α = 2.6, E_{max} = 10^{19} eV for PLE). Assumed values: maximum blazar activity time t_{max} = 6 months, magnetic field B = 10^{-16} G. Neutrino flux upper limits are indicated for a spectrum of dN/dE ∝ E^{-2}, matching the IceCube detection IC-170922A.

Proton Cascade/Spectrum Modeling

We simulate the development of proton cascades in the intergalactic medium using the CRPropa Monte Carlo package [10]. The simulations include all relevant interactions, considering only cascade photons arriving within a 6-month blazar activity period. We convert the simulations into energy-dependent sky maps, which serve as input templates for data analysis, assuming the jet axis aligns precisely with the line of sight. For each magnetic field strength, we performed 1000 independent simulations and combined them into a single spectrum, focusing here on results for an intergalactic magnetic field strength of **B=10^{-16} G**. Proton injection is modeled using a power law with low and high energy exponential cut-offs:

$$\frac{dN_{\mathrm{casc}}}{dE_p} = \kappa E_p{}^{-\alpha_p} \exp\left(-\frac{E_{\mathrm{p,\,min}}}{E_p}\right) \exp\left(-\frac{E_p}{E_{\mathrm{p,\,max}}}\right)$$

The low energy cut-off is fixed at $E_{p,min}$=10^{13} eV, constrained by the total proton luminosity of TXS 0506+056. The spectral slope α_p ranges from 1.8 to 2.6, and the high energy cut-off $E_{p,max}$ varies between 10^{14} and 10^{19} eV.

The primary gamma-ray spectrum is modeled as either a log parabola (LP) or a power law with an exponential cutoff (PLE), respectively, both attenuated by the Extragalactic Background Light:

$$\frac{dN_{\mathrm{prim}}}{dE_\gamma} = N_0 \left(\frac{E_\gamma}{E_0}\right)^{-\Gamma_{\mathrm{LP}} - \beta \ln\left(\frac{E_\gamma}{E_0}\right)} \exp(-\tau_{\gamma\gamma})$$

$$\frac{dN_{\mathrm{prim}}}{dE_\gamma} = N_0 \left(\frac{E_\gamma}{E_0}\right)^{-\Gamma_{\mathrm{PLE}}} \exp\left(-\frac{E_\gamma}{E_{\gamma,\mathrm{cut}}}\right) \exp(-\tau_{\gamma\gamma})$$

We combine this primary spectrum with the proton cascade component to match the observed *Fermi*-LAT and VERITAS spectra. The fit is evaluated using the χ^2 minimization technique across a grid of proton injection parameters using the MINUIT fit routine in gammapy, with 10^{-16} G ≤ B ≤ 10^{-14} G and the EBL model from Domínguez A., et al., 2011 [11].

Proton Model Constraints

We constrain the spectrum of protons escaping TXS 0506+056 by fitting the combined *Fermi*-LAT and VERITAS spectra with two models using gammapy: LP+EBL and PLE+EBL in figure 2. The LP+EBL model describes the gamma-ray data adequately without the cascade component (both χ^2=19.5), while the PLE+EBL model shows significant improvement with its inclusion, suggesting a better alignment with observations (**χ^2=30.4 → 24.9**).

Simulated neutrino spectra for these proton parameters remain within the upper limits of the observed neutrino flux, supporting the consistency of the proton cascade scenario with current data.

To refine the constraints, we analyzed the fit quality across a grid of proton injection parameters, focusing on the spectral slope α_p and high-energy cutoff $E_{p,max}$ for our fixed magnetic field in figure 3. The resulting statistical surfaces reveal regions of parameter space incompatible with the gamma-ray data, as indicated by 1σ and 2σ contours. The analysis also highlights areas of equal proton escape luminosity, further narrowing down the range of viable proton injection parameters and providing a clearer understanding of the proton spectrum that best fits the observations.

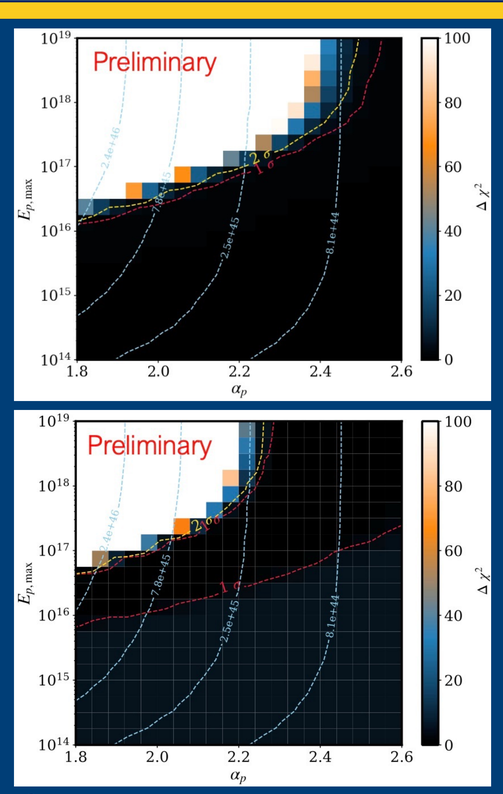

Figure 3: Results of the fit for the proton spectrum parameters, assuming an LP primary spectrum (above) and a PLE primary spectrum (below). The analysis is conducted under the assumption of a maximum blazar activity time of 6 months and a magnetic field of B=10^{-16}G. The color scale denotes the difference in χ^2 values obtained at each point and the minimum χ^2 obtained over the entire parameter space. The dashed yellow curve illustrates the 2σ uncertainty contours, while the dashed blue curves denote points within the parameter space corresponding to the same proton escape luminosity.

References

[1] Aartsen M. G., et al., 2014, Phys. Rev. Lett., 113, 101101
[2] Aartsen M. G., et al., 2018, Advances in Space Research, 62, 2902
[3] Kopper C., Blaufuss E., 2017, GRB Coordinates Network, 21916, 1
[4] The IceCube Collaboration et al., 2018, Science, 361
[5] Essey W., Kusenko A., 2010, Astroparticle Physics, 33, 81
[6] Abeysekara A. U., et al., 2018, ApJL, 861, L20
[7] Jin W., et al., 2022, 37th International Cosmic Ray Conference, 945
[8] Wood M., et al., 2017, 35th International Cosmic Ray Conference, 824
[9] NASA HEASARC, 2014, Astrophysics Source Code Library, ascl:1408.004
[10] Alves Batista R., et al., 2016b, JCAP, 2016, 038
[11] Domínguez A., et al., 2011, MNRAS, 410, 2556